International Journal of Engineering & Applied Sciences (IJEAS)
Vol.6, Issue4(2014)52-67

SHAPE EFFECT ON FREE VIBRATION OF FUNCTIONALLY GRADED PLATES

Hasan Kurtaran

Department of Mechanical Engineering, Gebze Technical University, Gebze-Kocaeli, Turkey
E-mail address: hasan@gyte.edu.tr

Received date: April 2014
Accepted date: December 2014

Abstract

In this article, shape effect on free vibration behavior of functionally graded plates is investigated. Square, rectangular, skew, circular, elliptical, annular and equilateral triangular plates with the same surface area and thickness are considered. Frequency values of these plates are compared for simply supported and clamped boundary conditions. Finite element method (FEM) is used in calculating frequency values and mode shapes. Since commercial codes do not allow inputting functionally graded material properties directly, MATLAB code was developed for FEM solution. Findings of this study can be useful for designers that have freedom to choose the plate shape in engineering applications.

Keywords: Free Vibration, Plate, Functionally Graded Material, Finite Element Analyses.

1. Introduction

Functionally graded materials (FGMs) were developed to overcome problems such as high thermal residual stresses and stress concentrations at the interface of conventional composite materials. FGMs are obtained by combining different sets of materials commonly metal with ceramic. In FGMs desirable mechanical properties are achieved by changing volume fraction gradually through the thickness. Mechanical properties in FGMs are expressed with various mathematical functions such as power law form of distribution.

Due to importance, bending, vibration, buckling etc. behavior of FGM plates received great attention in the last decade. Many studies were conducted to investigate the free vibration behavior of various plate shapes such as rectangular, skew, circular, elliptical and annular plates. Yang et al. [1] investigated the dynamic response of initially stressed functionally graded rectangular thin plates subjected to partially distributed impulsive lateral loads. Hosseini et al. [2, 3] obtained closed form solution of moderately thick and thick rectangular FGM plates for free vibration. Sheikholeslami et al. [4] investigated free vibration of functionally graded thick rectangular plates with an analytical approach. Huang et al. [5] investigated three-dimensional (3-D) vibrations of rectangular parallelepipeds of functionally graded material with Ritz method. Latifi et al. [6] investigated buckling of thin rectangular functionally graded plates. Kim, Y. W. [7] investigated vibration characteristics of initially stressed functionally graded rectangular plates in thermal environment with the Rayleigh–Ritz procedure. Sundararajana et al. [8] investigated free vibration characteristics of functionally graded material rectangular and skew plates subjected to thermal environment analytically and numerically. Upadhyay et al. [9] investigated nonlinear static and dynamic behavior of functionally graded skew plates. Singha et al. [10] investigated the large amplitude free flexural vibration behavior of symmetrically laminated composite skew plates using the finite

element method. Ganapathia et al. [11] investigated thermal buckling of functionally graded skew plate with the finite element approach. Nie et al. [12] investigated the three-dimensional free and forced vibration analysis of functionally graded circular plate for various boundary conditions with semi-analytical approach. Allahverdizadeh et al. [13, 14] employed a semi-analytical approach for nonlinear free and forced axisymmetric vibration of a thin circular functionally graded plate. Zhu et al. [15] investigated free vibration analysis of functionally graded circular plates in thermal environments with a local Kriging meshless method. Talabi et al. [16] investigated free vibration of thick circular FGM plates analytically. Matsunaga H. [17] investigated vibration and buckling of FGM circular cylindrical shells. Hosseini-Hashemi et al. [18] investigated closed-form solution of frequency equation for free vibration analysis of circular/annular moderately thick FGM plates. Patel et al. [19] investigated the free vibration characteristics of functionally graded elliptical cylindrical shells using finite element. Hsieh et al. [20] investigated static behavior of FGM elliptical plate using approximation method. Zhang D-G. [21] investigated non-linear bending analysis for super elliptical thin plates with Ritz method. Ceribasi et al. [22] investigated static behavior of clamped superelliptical plates with Galerkin's method. Nie et al. [23] investigated free and forced vibration of functionally graded annular sectorial plates using a semi-analytical approach. Nie et al. [24] investigated dynamic analysis of multi-directional functionally graded annular plates using a semi-analytical numerical method. Hosseini-Hashemi et al. [25] investigated an analytical solution for free vibration analysis of stepped circular and annular FG plates. Jodaeia et al. [26] investigated three-dimensional vibration analysis of functionally graded annular plates using state-space based differential quadrature method. Ebrahimi et al. [27] investigated free vibration analysis of moderately thick annular functionally graded plate with piezoelectric layers. Tajeddini et al. [28] investigated free vibration analysis of thick circular and annular functionally graded plates with variable thickness using elasticity theory. Belalia et al. [29] investigated nonlinear free vibration analysis of functionally graded sector plates with p-version of the finite element.

Regarding vibration of triangular FGM plates, to the author’s knowledge no study is available. In this study free vibration behavior of various FGM plates is analyzed. Frequencies of square, rectangular, skew, circular, elliptical, annular plates as well as equilateral triangular plate are calculated and compared with each other for simply support and clamped boundary conditions. In the analytical studies of FGM plates, often Poisson’s ratio is assumed to be constant in contrast to elastic modulus and density to make solution easier. In this study, this limitation is also overcome by using FEM and numerical integration procedures.

2. FINITE ELEMENT EQUATION FOR FREE VIBRATION

2.1 Displacements and Strains

In this study, free vibration analyses of square, rectangular, skew, circular, elliptical, annular and equilateral triangular plates are carried out with FEM. Free vibration analyses are conducted using 4-node quadrilateral shell element shown in Fig. (1). For a 4-node quadrilateral shell element stiffness and mass matrices that are needed in modal analyses are derived as following.

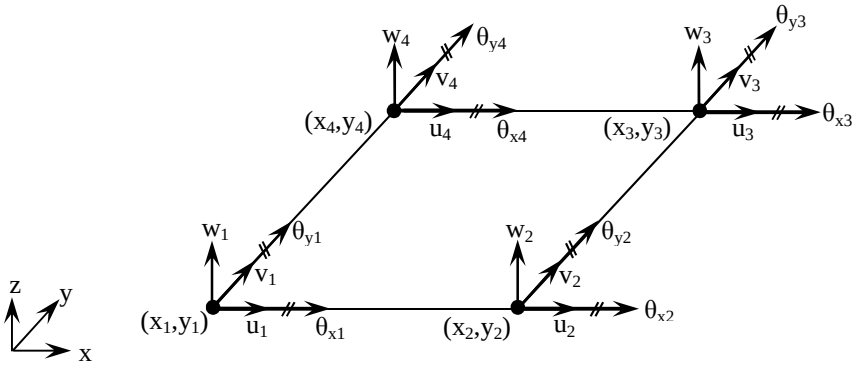

Figure 1: 4-node quadrilateral shell element.

Displacements at a general point (x, y, z) in a shell element as shown in Fig. (1) can be stated as

$$\begin{aligned} u(x,y,z) &= u_0(x,y) + z\theta_x(x,y) \\ v(x,y,z) &= v_0(x,y) + z\theta_y(x,y) \\ w(x,y,z) &= w_0(x,y) \end{aligned} \tag{1}$$

where u_0, v_0, w_0 are displacements of mid-plane of the shell in x, y, z directions respectively and θx, θy are rotations of mid-plane in x-z and y-z plane respectively.

For thick plates using First Order Shear Deformation Theory (FSDT), strain-displacement relationships can be written as

$$\begin{Bmatrix} \varepsilon_{xx} \\ \varepsilon_{yy} \\ \gamma_{xy} \\ \gamma_{yz} \\ \gamma_{zx} \end{Bmatrix} = \begin{Bmatrix} \varepsilon_{xx}^{(0)} \\ \varepsilon_{yy}^{(0)} \\ \gamma_{xy}^{(0)} \\ \gamma_{yz}^{(0)} \\ \gamma_{zx}^{(0)} \end{Bmatrix} + z \begin{Bmatrix} \varepsilon_{xx}^{(1)} \\ \varepsilon_{yy}^{(1)} \\ \gamma_{xy}^{(1)} \\ \gamma_{yz}^{(1)} \\ \gamma_{zx}^{(1)} \end{Bmatrix} = \begin{Bmatrix} \dfrac{\partial u_0}{\partial x} \\ \dfrac{\partial v_0}{\partial y} \\ \dfrac{\partial u_0}{\partial y} + \dfrac{\partial v_0}{\partial x} \\ \dfrac{\partial w}{\partial y} + \theta_y \\ \dfrac{\partial w}{\partial x} + \theta_x \end{Bmatrix} + z \begin{Bmatrix} \dfrac{\partial \theta_x}{\partial x} \\ \dfrac{\partial \theta_y}{\partial y} \\ \dfrac{\partial \theta_x}{\partial y} + \dfrac{\partial \theta_y}{\partial x} \\ 0 \\ 0 \end{Bmatrix} \tag{2}$$

2.2 Equation of Motion

Free vibration equation can be obtained from the dynamic version of virtual work as

$$\delta U + \delta T = 0 \tag{3}$$

Where δU and δT indicate virtual work of internal and inertial forces respectively. Virtual work of internal forces in terms of stresses and strains in element domain A is given as [30].

$$\delta U = \int_A \left\{ \int_{-h/2}^{h/2} \begin{bmatrix} \sigma_{xx}\left(\delta\varepsilon_{xx}^{(0)} + z\,\delta\varepsilon_{xx}^{(1)}\right) + \sigma_{yy}\left(\delta\varepsilon_{yy}^{(0)} + z\,\delta\varepsilon_{yy}^{(1)}\right) + \sigma_{xy}\left(\delta\gamma_{xy}^{(0)} + z\,\delta\gamma_{xy}^{(1)}\right) + \\ \sigma_{yz}\delta\gamma_{yz}^{(0)} + \sigma_{zx}\delta\gamma_{zx}^{(0)} \end{bmatrix} dz \right\} dxdy \tag{4}$$

Eq. (4) can also be written in terms of stress resultants as

$$\delta U = \int_A \left\{ \int_{-h/2}^{h/2} \begin{bmatrix} N_{xx}\delta\varepsilon_{xx}^{(0)} + M_{xx}\delta\varepsilon_{xx}^{(1)} + N_{yy}\delta\varepsilon_{yy}^{(0)} + M_{yy}\delta\varepsilon_{yy}^{(1)} + N_{xy}\delta\gamma_{xy}^{(0)} + M_{xy}\delta\gamma_{xy}^{(1)} + \\ Q_y\delta\gamma_{yz}^{(0)} + Q_x\delta\gamma_{zx}^{(0)} \end{bmatrix} dz \right\} dxdy \tag{5}$$

Stress resultants (N_{xx}, N_{yy}, N_{xy}, M_{xx}, M_{yy}, M_{xy}, Q_x, Q_y) in Eq. (5) are defined as

$$\begin{Bmatrix} N_{xx} \\ N_{yy} \\ N_{xy} \end{Bmatrix} = \int_{-h/2}^{h/2} \begin{Bmatrix} \sigma_{xx} \\ \sigma_{yy} \\ \sigma_{xy} \end{Bmatrix} dz = \left[\int_{-h/2}^{h/2} C(z)dz \right] \begin{Bmatrix} \varepsilon_{xx}^{(0)} \\ \varepsilon_{yy}^{(0)} \\ \gamma_{xy}^{(0)} \end{Bmatrix} + \left[\int_{-h/2}^{h/2} C(z)zdz \right] \begin{Bmatrix} \varepsilon_{xx}^{(1)} \\ \varepsilon_{yy}^{(1)} \\ \gamma_{xy}^{(1)} \end{Bmatrix} = [A_m] \begin{Bmatrix} \varepsilon_{xx}^{(0)} \\ \varepsilon_{yy}^{(0)} \\ \gamma_{xy}^{(0)} \end{Bmatrix} + [B_m] \begin{Bmatrix} \varepsilon_{xx}^{(1)} \\ \varepsilon_{yy}^{(1)} \\ \gamma_{xy}^{(1)} \end{Bmatrix} \tag{6}$$

$$\begin{Bmatrix} M_{xx} \\ M_{yy} \\ M_{xy} \end{Bmatrix} = \int_{-h/2}^{h/2} \begin{Bmatrix} \sigma_{xx} \\ \sigma_{yy} \\ \sigma_{xy} \end{Bmatrix} zdz = \left[\int_{-h/2}^{h/2} C(z)zdz \right] \begin{Bmatrix} \varepsilon_{xx}^{(0)} \\ \varepsilon_{yy}^{(0)} \\ \gamma_{xy}^{(0)} \end{Bmatrix} + \left[\int_{-h/2}^{h/2} C(z)z^2dz \right] \begin{Bmatrix} \varepsilon_{xx}^{(1)} \\ \varepsilon_{yy}^{(1)} \\ \gamma_{xy}^{(1)} \end{Bmatrix} = [B_m] \begin{Bmatrix} \varepsilon_{xx}^{(0)} \\ \varepsilon_{yy}^{(0)} \\ \gamma_{xy}^{(0)} \end{Bmatrix} + [D_m] \begin{Bmatrix} \varepsilon_{xx}^{(1)} \\ \varepsilon_{yy}^{(1)} \\ \gamma_{xy}^{(1)} \end{Bmatrix} \tag{7}$$

$$\begin{Bmatrix} Q_y \\ Q_x \end{Bmatrix} = k_s \int_{-h/2}^{h/2} \begin{Bmatrix} \sigma_{yz} \\ \sigma_{zx} \end{Bmatrix} dz = \left[k_s \int_{-h/2}^{h/2} C_s(z)dz \begin{Bmatrix} \gamma_{yz}^{(0)} \\ \gamma_{zx}^{(0)} \end{Bmatrix} \right] = [Q_m] \begin{Bmatrix} \gamma_{yz}^{(0)} \\ \gamma_{zx}^{(0)} \end{Bmatrix} \tag{8}$$

In Eq. (6-7) **C** is material matrix for plane stress case and in Eq. (8) $\mathbf{C_s}$ is material matrix for transverse shear for functionally graded material. In Eq. (8) k_s is the shear correction factor and it is equal to (5/6) for rectangular sections.

Virtual work of inertial forces is expressed as

$$\delta T = \int_A \left\{ \int_{-h/2}^{h/2} \rho(z) \left[\left(\ddot{u}_0 + z\,\ddot{\theta}_x \right)\left(\delta u_0 + z\,\delta\theta_x\right) + \left(\ddot{v}_0 + z\,\ddot{\theta}_y \right)\left(\delta v_0 + z\,\delta\theta_y\right) + \ddot{w}\,\delta w \right] dz \right\} dxdy \tag{9}$$

where ρ indicates the density of functionally graded material. Material properties vary in thickness direction in functionally graded materials. In finite element method displacement and rotations within the element are obtained through the following interpolation functions;

$$\begin{aligned} u_0 &= \sum_{i=1}^{4} N_i(x,y)u_i \qquad & \theta_x &= \sum_{i=1}^{4} N_i(x,y)\theta_{xi} \\ v_0 &= \sum_{i=1}^{4} N_i(x,y)v_i & \theta_y &= \sum_{i=1}^{4} N_i(x,y)\theta_{yi} \\ w_0 &= \sum_{i=1}^{4} N_i(x,y)w_i \end{aligned} \tag{10}$$

where Ni indicate shape functions and u_i, v_i, w_i, θ_{xi}, θ_{yi} are nodal displacement and rotations. If nodal displacement and rotations of the element are denoted as the vector of $u_e^T = \{u_1, v_1, w_1, .\theta_{x1}, \theta_{y1}, ..., u_4, v_4, w_4, .\theta_{x4}, \theta_{y4}\}$, in-plane and transverse shear strains can be written in terms of nodal displacement vector as

$$\begin{Bmatrix} \varepsilon_{xx}^{(0)} \\ \varepsilon_{yy}^{(0)} \\ \gamma_{xy}^{(0)} \end{Bmatrix} = B_0 u_e \tag{11}$$

$$\begin{Bmatrix} \varepsilon_{xx}^{(1)} \\ \varepsilon_{yy}^{(1)} \\ \gamma_{xy}^{(1)} \end{Bmatrix} = B_1 u_e \tag{12}$$

$$\begin{Bmatrix} \gamma_{yz}^{(0)} \\ \gamma_{zx}^{(0)} \end{Bmatrix} = B_s u_e \tag{13}$$

where $\mathbf{B_0}$, $\mathbf{B_1}$ and $\mathbf{B_s}$ matrices are given in terms of shape function derivatives as

$$B_0 = \begin{bmatrix} N_{1,x} & 0 & 0 & 0 & 0 & \cdots & \cdots & N_{4,x} & 0 & 0 & 0 & 0 \\ 0 & N_{1,y} & 0 & 0 & 0 & \cdots & \cdots & 0 & N_{4,y} & 0 & 0 & 0 \\ N_{1,y} & N_{1,x} & 0 & 0 & 0 & \cdots & \cdots & N_{4,y} & N_{4,x} & 0 & 0 & 0 \end{bmatrix} \tag{14}$$

$$B_1 = \begin{bmatrix} 0 & 0 & 0 & N_{1,x} & 0 & \cdots & \cdots & 0 & 0 & 0 & N_{4,x} & 0 \\ 0 & 0 & 0 & 0 & N_{1,y} & \cdots & \cdots & 0 & 0 & 0 & 0 & N_{4,y} \\ 0 & 0 & 0 & N_{1,y} & N_{1,x} & \cdots & \cdots & 0 & 0 & 0 & N_{4,y} & N_{4,x} \end{bmatrix} \tag{15}$$

$$B_s = \begin{bmatrix} 0 & 0 & N_{1,y} & 0 & N_1 & \cdots & \cdots & 0 & 0 & N_{4,x} & 0 & N_4 \\ 0 & 0 & N_{1,x} & N_1 & 0 & \cdots & \cdots & 0 & 0 & N_{4,x} & N_4 & 0 \end{bmatrix} \tag{16}$$

Using the aforementioned equations and virtual work definition, stiffness **K** and mass **M** matrices for quadrilateral shell element are written as

$$K = \int \left[B_0^T \left(A_m B_0 + B_m B_1 \right) + B_1^T \left(B_m B_0 + D_m B_1 \right) dA dz + B_S^T Q_m B_S \right] dx dy \tag{17}$$

$$M = \int_A \left\{ \int_{-h/2}^{h/2} \rho \left(X_1^T X_0^T \right) \left(X_0 X_1 \right) dz \right\} dx dy \tag{18}$$

$\mathbf{X_0}$ matrix in Eq. (18) is given as

$$X_0 = \begin{bmatrix} 1 & 0 & 0 & z & 0 \\ 0 & 1 & 0 & 0 & z \\ 0 & 0 & 1 & 0 & 0 \end{bmatrix} \tag{19}$$

and $\mathbf{X_1}$ matrix in Eq. (18) is given as

$$X_1 = \begin{bmatrix} N_1 & 0 & 0 & 0 & 0 & \cdots & N_4 & 0 & 0 & 0 & 0 \\ 0 & N_1 & 0 & 0 & 0 & \cdots & 0 & N_4 & 0 & 0 & 0 \\ 0 & 0 & N_1 & 0 & 0 & \cdots & 0 & 0 & N_4 & 0 & 0 \\ 0 & 0 & 0 & N_1 & 0 & \cdots & 0 & 0 & 0 & N_4 & 0 \\ 0 & 0 & 0 & 0 & N_1 & \cdots & 0 & 0 & 0 & 0 & N_4 \end{bmatrix} \tag{20}$$

Using the derived stiffness and mass matrices, free vibration equation is given as

$$M \ddot{U} + KU = 0 \tag{21}$$

where $\ddot{U}$ and U indicate nodal accelerations and displacements respectively. Since mass and stiffness matrices are higher order function of x, y and z, they are often calculated numerically, e.g. using Gauss Quadrature rule. In numerical integration full integration is applied to mass matrix as well as to the in-plane terms of stiffness matrices while reduced integration is applied to the transverse shear terms of the stiffness matrix.

In free vibration, frequencies are solved from the following eigenvalue problem

$$\left[-\omega^2 M + K \right] U = 0 \tag{22}$$

where ω indicates the frequency value. In this study eigenvalue problem is solved by Matrix Iteration Method [21].

Since commercial FEM codes do not allow directly inputting FGM properties, a FEM computer code was developed to implement finite element method and solve frequency equation. Developed program was validated with the analytical results for free vibration of circular and annular FGM plates in Hashemi et al. article [22].

3. FREE VIBRATION ANALYSIS

In this section, modal analyses of square, rectangular, skew, circular, elliptical, annular and equilateral triangular FGM plates shown in Fig. (2) are conducted for simply support and clamped boundary conditions. For a fair comparison the same surface area of 100 m^2 and thickness value of 0.1 m were used for all FGM plates in this study. Characteristic dimensions of plates are shown in Fig. (2) and their specific values are given as following.

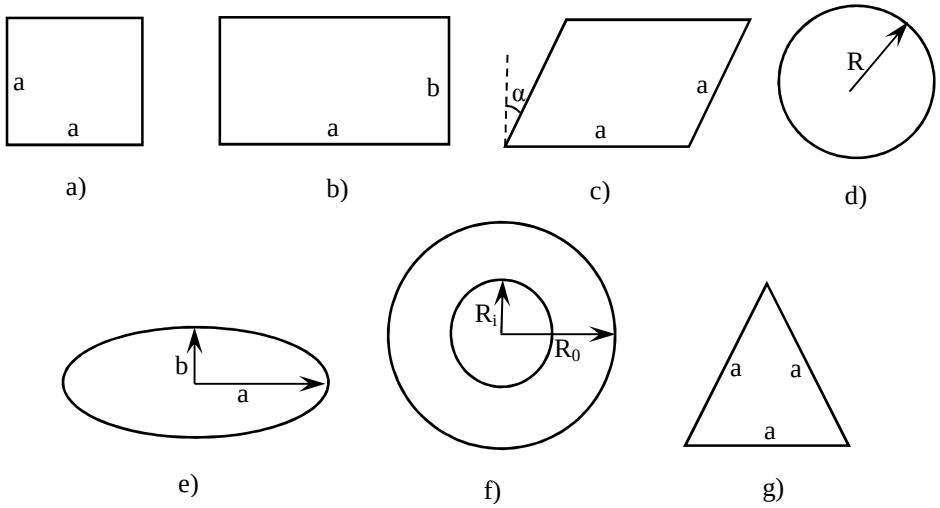

Figure 2: Plate shapes: a) Square, b) Rectangle, c) Skew, d) Circular, e) Elliptic, f) Annular, g) Triangular

In Fig. (2) a and b indicate side lengths in square, rectangle, skew and triangular plates. R indicates radius of circular plate. Ri and Ro indicate inner and outer radius of annular plate. In square plate a=10 m, in rectangular plate a=14.142 m and b=a/2, in skew plate a=10.745 m and skewness angle α=30°, in circular plate R=5.641 m, in elliptic plate a=7.9788 m and b=a/2, in annular plate Ro=6.514 m and Ri = Ro/2, in equilateral triangular plate a=15.196 m.

In FGMs, material property such as elastic modulus, Poisson's ratio and density change in thickness direction. Material property at a distance z within the thickness can be given by a power law distribution function as below

$$P(z) = \left(P_c - P_m\right)\left(\frac{z}{h} + \frac{1}{2}\right)^n + P_m \tag{23}$$

where P_c and P_m are material properties for ceramic and metal materials respectively, n is the volume fraction exponent of the FGM and h is the thickness of the plate. FGM material properties given in Table 1 along with the parameter value of n=2 are used in this study.

Table 1: FGM material properties.

	Ceramic	*Aluminum*
Elastic modulus (GPa)	390	70
Poisson's ratio	0.26	0.34
Density (kg/m^3)	3900	2700

In free vibration analyses, for simply support boundary condition, only nodal displacements at boundaries are constrained as below

$$u_i = v_i = w_i = 0 \tag{24}$$

For clamped boundary condition, both nodal displacements and rotations at boundaries are constrained as below

$$u_i = v_i = w_i = \theta_{xi} = \theta_{yi} = 0 \tag{25}$$

Frequency values of FGM plates for six mode shapes are given in Tables 2-3 and corresponding mode shapes are shown in Fig. (3-16). To save space only three mode shapes are shown in figures. In Fig. (3-16) SSSS, SSSS, SSSS, S, S, SS, SSS indicate clamped boundary condition for square, rectangular, skew, circular, elliptic, annular and triangular respectively. CCCC, CCCC, CCCC, C, C, CC, CCC indicate simply supported boundary condition for square, rectangular, skew, circular, elliptic, annular and triangular respectively.

Normalized frequency values for six mode shapes are given in Tables 4-5. For simply supported boundary condition, it is seen from Table 2 that annular plate has the highest frequency value followed by rectangular-triangular-skew-elliptic-square-circular plates for Mode 1 shape. For Mode 2, annular plate has the highest frequency value followed by triangular-square-skew- circular-rectangular-elliptic plates. For Mode 3, annular plate has the highest frequency value followed by rectangular-skew-elliptic-triangular-square-circular plates. For Mode 4, annular plate has the highest frequency value followed by triangular-rectangular-circular-square-elliptic-skew plates. For Mode 5, annular plate has the highest frequency value followed by skew-square-rectangular-triangular-circular-elliptic plates. For Mode 6, annular plate has the highest frequency value followed by circular-triangular-square-elliptic-rectangular-skew plates.

For clamped boundary condition, it is seen from Table 3 that annular plate has the highest frequency value followed by rectangular-elliptic-triangular-skew-square-circular plates for Mode 1 shape. For Mode 2, annular plate has the highest frequency value followed by triangular-square-skew-circular-rectangular-elliptic plates. For Mode 3, annular plate has the highest frequency value followed by skew-rectangular-elliptic-triangular-square-circular plates. For Mode 4, annular plate has the highest frequency value followed by triangular-rectangular-circular-elliptic-square-skew plates. For Mode 5, annular plate has the highest frequency value followed by skew-triangular-square-rectangular-circular-elliptic plates. For Mode 6, annular plate has the highest frequency value followed by triangular-circular-rectangular-square-elliptic-skew plates.

Also from Table 6 it is clear that when boundary condition is changed from simply supported to clamped, frequencies increase. Increase is the highest for Mode 1 and is getting lower towards Mode 6.

Table 2: Frequency values of plates for simply supported boundary condition.

Frequency Values (Hz) (Simply Supported Boundary Condition)							
Mode Numbers	*Square*	*Rectangular*	*Skew*	*Circular*	*Elliptic*	*Annular*	*Triangular*
Mode 1	7.22	9.06	7.88	5.75	7.68	35.28	8.34
Mode 2	16.97	13.94	15.87	14.82	13.02	36.43	18.43
Mode 3	16.97	22.25	21.25	14.82	20.89	36.51	18.44
Mode 4	27.25	28.43	25.25	27.45	24.47	40.12	31.70
Mode 5	34.04	33.99	36.93	32.03	31.07	46.62	33.92
Mode 6	44.04	42.42	41.81	51.75	43.95	127.90	49.64

Table 3: Frequency values of plates for clamped boundary condition.

Frequency Values (Hz) (Clamped Boundary Condition)							
Mode Numbers	*Square*	*Rectangular*	*Skew*	*Circular*	*Elliptic*	*Annular*	*Triangular*
Mode 1	12.11	16.54	13.44	10.81	14.48	71.13	14.42
Mode 2	24.76	21.45	23.87	22.52	20.93	71.90	27.57
Mode 3	24.76	30.26	30.74	22.60	29.81	71.98	27.57
Mode 4	36.51	43.12	34.94	37.06	37.00	74.62	43.13
Mode 5	44.78	43.15	48.50	42.36	41.09	78.69	46.05
Mode 6	55.82	59.73	54.58	64.99	55.19	198.24	69.82

Table 4: Frequency values for various plates for simply supported boundary conditions.

Normalized Frequency Values (Simply Supported Boundary Condition)							
Mode Numbers	*Square*	*Rectangular*	*Skew*	*Circular*	*Elliptic*	*Annular*	*Triangular*
Mode 1	1.25	1.58	1.37	1.00	1.34	6.14	1.45
Mode 2	1.30	1.07	1.22	1.14	1.00	2.80	1.42
Mode 3	1.15	1.49	1.43	1.00	1.41	2.46	1.24
Mode 4	1.11	1.16	1.03	1.12	1.00	1.64	1.30
Mode 5	1.10	1.10	1.19	1.03	1.00	1.50	1.09
Mode 6	1.05	1.01	1.00	1.24	1.05	3.05	1.19

Table 5: Frequency values for various plates for clamped boundary conditions.

Normalized Frequency Values (Clamped Boundary Condition)							
Mode Numbers	*Square*	*Rectangular*	*Skew*	*Circular*	*Elliptic*	*Annular*	*Triangular*
Mode 1	1.12	1.53	1.24	1.00	1.34	6.58	1.33
Mode 2	1.18	1.02	1.14	1.08	1.00	3.44	1.32
Mode 3	1.10	1.34	1.36	1.00	1.32	3.18	1.22
Mode 4	1.04	1.23	1.00	1.06	1.06	2.14	1.23
Mode 5	1.09	1.05	1.18	1.03	1.00	1.92	1.12
Mode 6	1.02	1.09	1.00	1.19	1.01	3.63	1.28

Table 6: Increase in frequency values when boundary condition is changed from simply supported to clamped.

Increase in Frequency Values (%)							
Mode Numbers	*Square*	*Rectangular*	*Skew*	*Circular*	*Elliptic*	*Annular*	*Triangular*
Mode 1	67.73	82.56	70.56	88.00	88.54	101.62	72.90
Mode 2	45.90	53.87	50.41	51.96	60.75	97.36	49.59
Mode 3	45.90	36.00	44.66	52.50	42.70	97.15	49.51
Mode 4	33.98	51.67	38.38	35.01	51.21	85.99	36.06
Mode 5	31.55	26.95	31.33	32.25	32.25	68.79	35.76
Mode 6	26.75	40.81	30.54	25.58	25.57	55.00	40.65

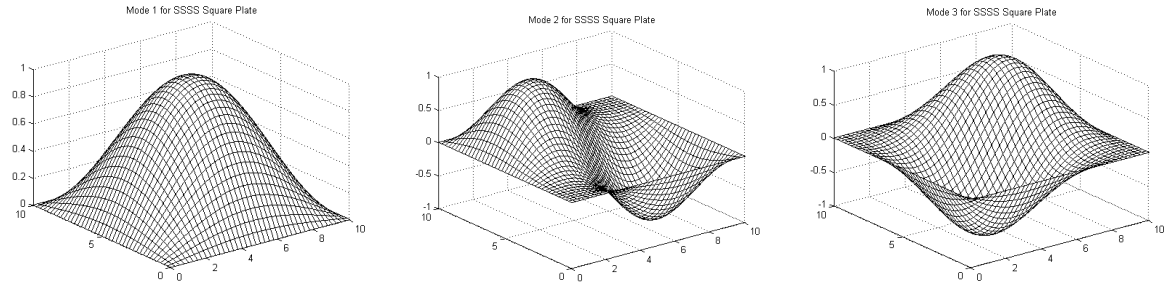

-a- -b- -c-

Figure 3: Mode shapes for simple support square plate a) Mode1, b) Mode 2, c) Mode 3

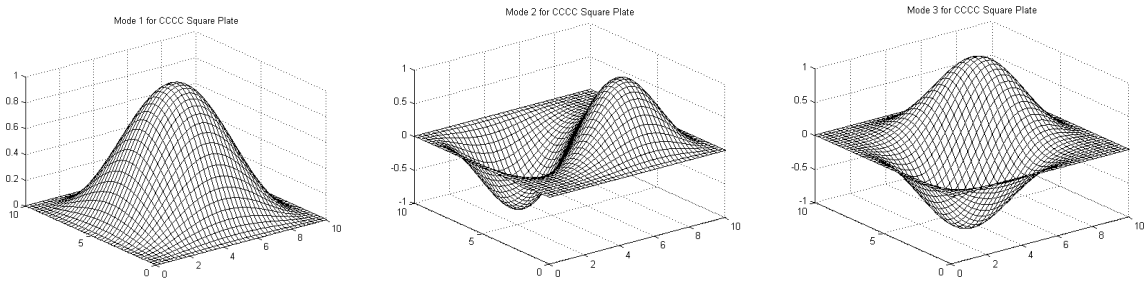

-a- -b- -c-

Figure 4: Mode shapes for clamped square plate a) Mode1, b) Mode 2, c) Mode 3

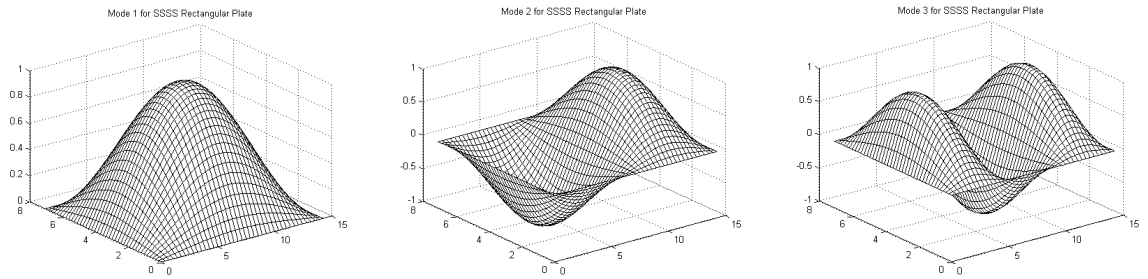

-a- -b- -c-

Figure 5: Mode shapes for simple support rectangular plate a) Mode1, b) Mode 2, c) Mode 3

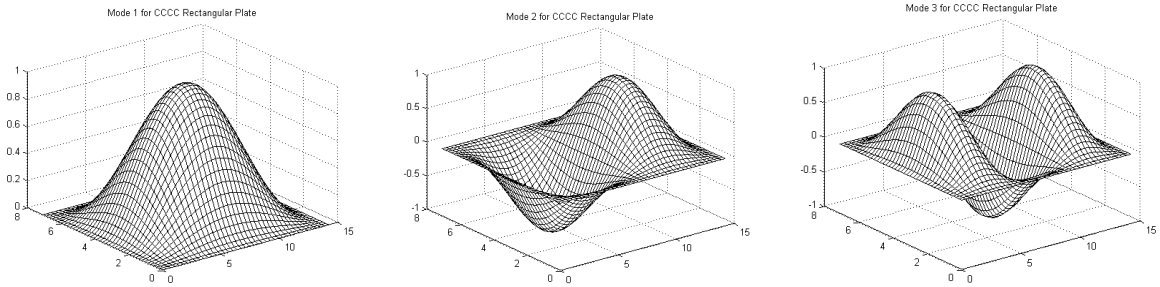

-a- -b- -c-

Figure 6: Mode shapes for clamped rectangular plate a) Mode1, b) Mode 2, c) Mode 3

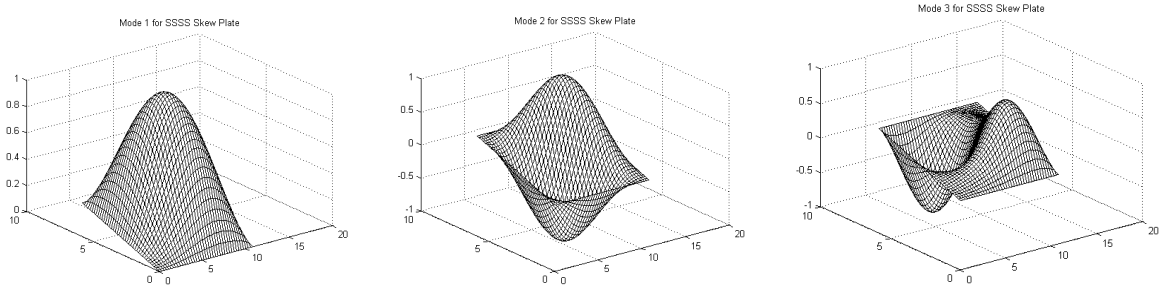

-a- -b- -c-

Figure 7: Mode shapes for simple support skew plate a) Mode1, b) Mode 2, c) Mode 3

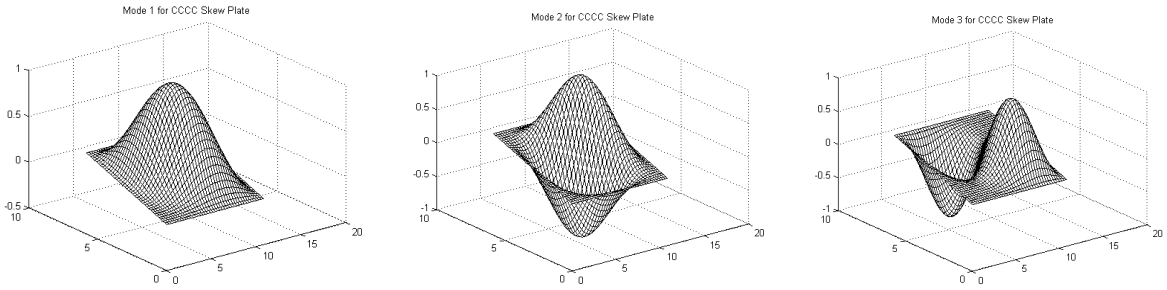

-a- -b- -c-

Figure 8: Mode shapes for clamped skew plate a) Mode1, b) Mode 2, c) Mode 3

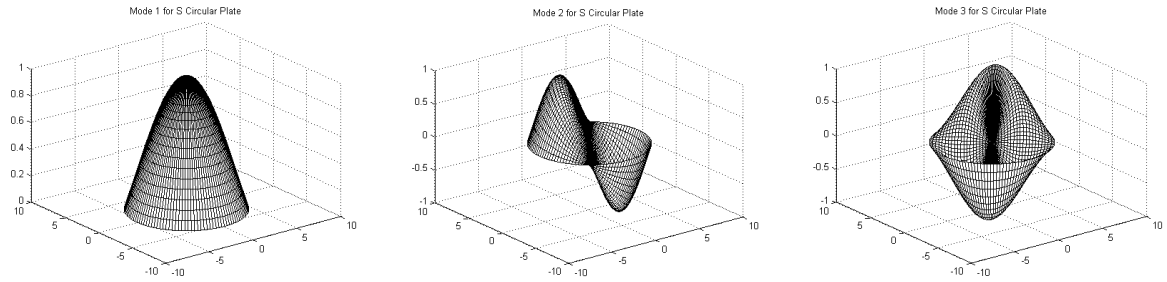

-a- -b- -c-

Figure 9: Mode shapes for simple support circular plate a) Mode1, b) Mode 2, c) Mode 3

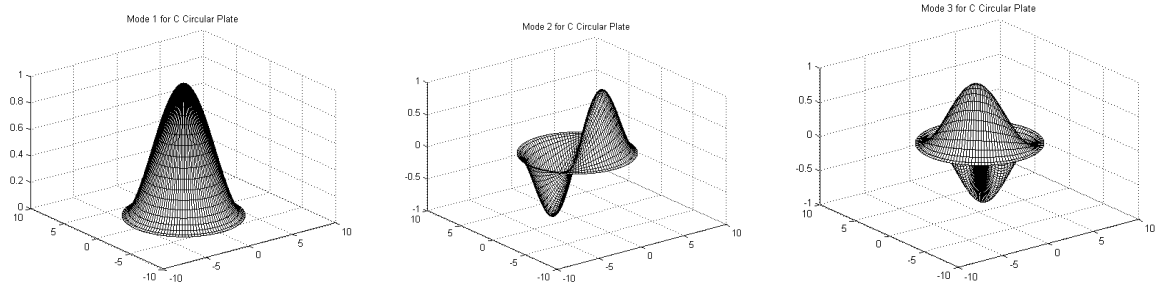

-a- -b- -c-

Figure 10: Mode shapes for clamped circular plate a) Mode1, b) Mode 2, c) Mode 3

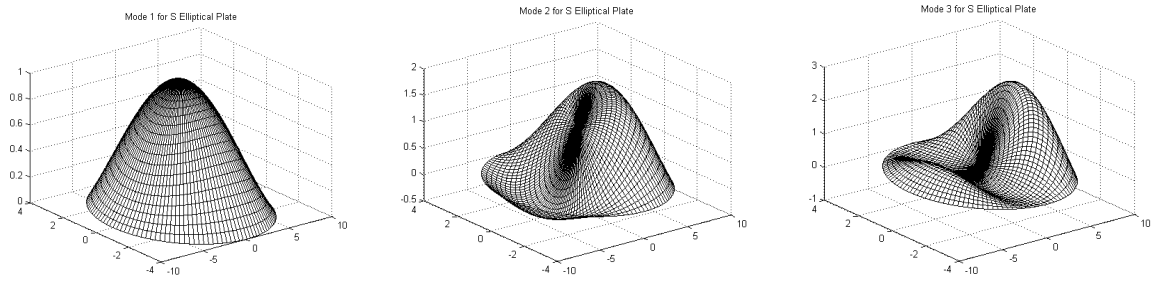

-a- -b- -c-

Figure 11: Mode shapes for simple support elliptic plate a) Mode1, b) Mode 2, c) Mode 3

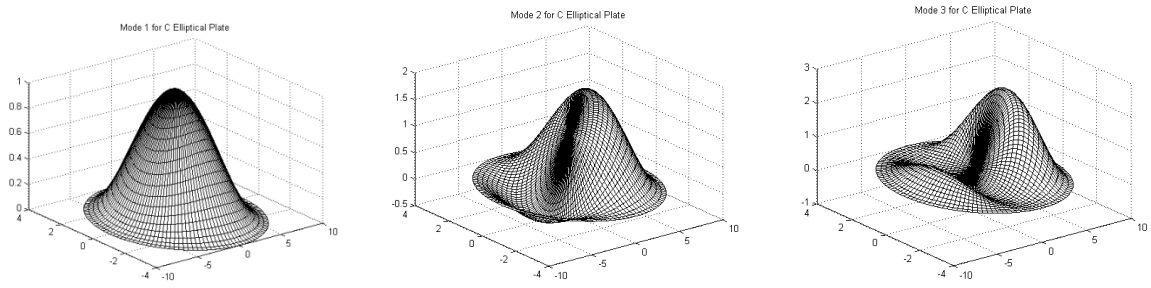

-a- -b- -c-

Figure 12: Mode shapes for clamped elliptic plate a) Mode1, b) Mode 2, c) Mode 3

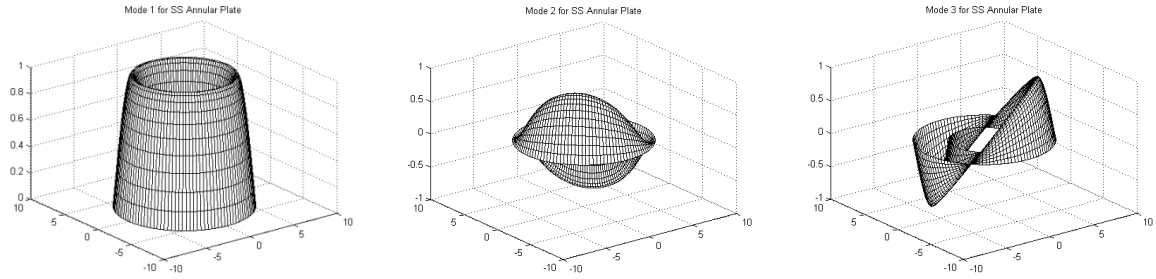

-a- -b- -c-

Figure 13: Mode shapes for simple support annular plate a) Mode1, b) Mode 2, c) Mode 3

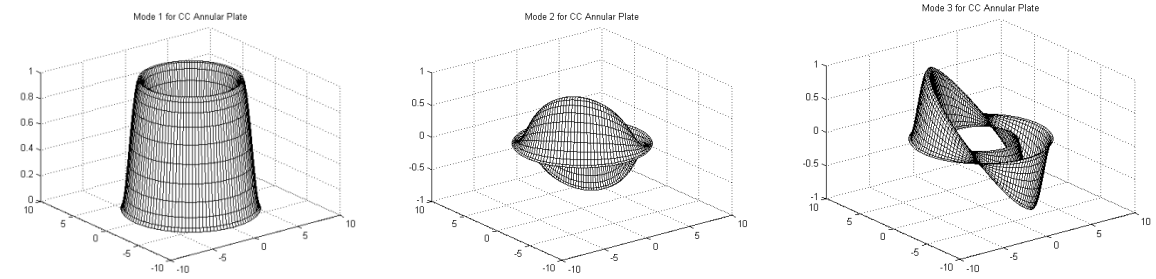

-a- -b- -c-

Figure 14: Mode shapes for clamped annular plate a) Mode1, b) Mode 2, c) Mode 3

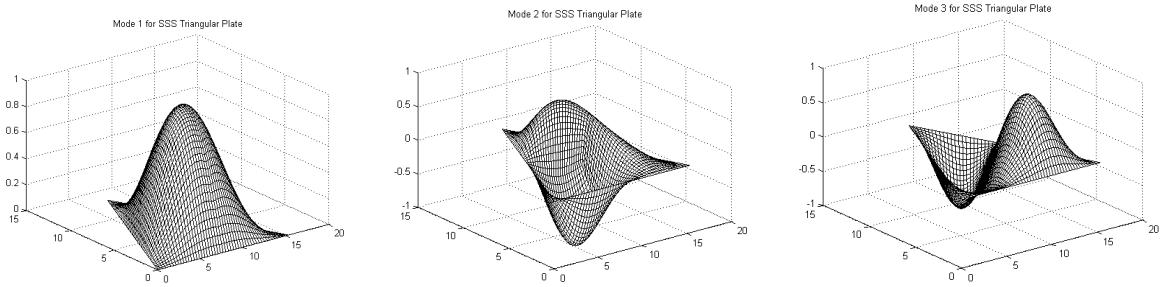

-a- -b- -c-

Figure 15: Mode shapes for simple support triangular plate a) Mode1, b) Mode 2, c) Mode 3

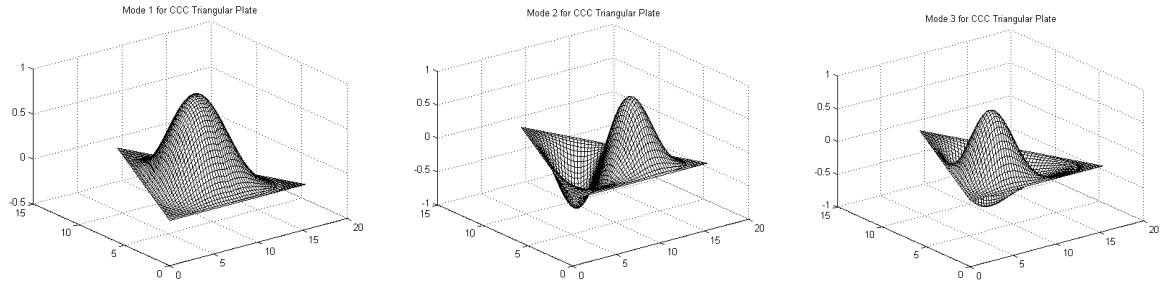

-a- -b- -c-

Figure 16: Mode shapes for clamped triangular plate: a) Mode1, b) Mode 2, c) Mode 3

4. CONCLUSION

In this study, shape effect on free vibration behavior of functionally graded plates is investigated. Square, rectangular, skew, circular, elliptical, annular and equilateral triangular plates with the same surface area and thickness are considered. Frequency values for simply supported and clamped boundary conditions are compared for lowest six vibration modes.

For simply supported and clamped boundary conditions annular plate has the highest frequency values. Frequency values of annular plate are about 5-7 times higher than those of other FGM plates. Although circular plate has the lowest frequency values, there is no significant difference in frequency values of square, rectangular, skew, circular, elliptical and equilateral triangular FGM plates.

Also it is observed that when boundary condition is changed from simply supported to clamped, frequency values increase. Increase in frequency values is the highest for Mode 1 and is getting lower towards Mode 6. That is the type of boundary condition has most effect on frequency values of lowest modes. Values of higher modes are less affected. Outcome of this study can be useful for designers that have freedom to choose the plate shape in engineering applications.

REFERENCES

[1] Yang, J. and Shen, H. S., Dynamic response of initially stressed functionally graded rectangular thin plates, *Composite Structures*, 54(4), 497-508, 2001.

[2] Hosseini-Hashemi, Sh., Fadaee, M. and Atashipour, S.R., A new exact analytical approach for free vibration of Reissner–Mindlin functionally graded rectangular plates, *International Journal of Mechanical Sciences*, 53(1), 11-22, 2011.

[3] Hosseini-Hashemi, Sh., Fadaee, M. and Atashipour, S.R., Study on the free vibration of thick functionally graded rectangular plates according to a new exact closed-form procedure, *Composite Structures*, 93(2), 722-735, 2011.

[4] Sheikholeslami, S.A. and Saidi, A.R., Vibration analysis of functionally graded rectangular plates resting on elastic foundation using higher-order shear and normal deformable plate theory, *Composite Structures*, 106, 350-361, 2013.

[5] Huang, C.S., McGee, III O.G. and Wang, K.P., Three-dimensional vibrations of cracked rectangular parallelepipeds of functionally graded material, *International Journal of Mechanical Sciences*, 70, 1-25, 2013.

[6] Latifi, M., Farhatnia, F. and Kadkhodaei, M., Buckling analysis of rectangular functionally graded plates under various edge conditions using Fourier series expansion, *European Journal of Mechanics-A/Solids*, 41, 16–27, 2013.

[7] Kim, Y. W., Temperature dependent vibration analysis of functionally graded rectangular plates, *Journal of Sound and Vibration*, 284(3-5), 531–549, 2005.

[8] Sundararajana, N., Prakashb, T. and Ganapathic, M., Nonlinear free flexural vibrations of functionally graded rectangular and skew plates under thermal environments, *Finite Elements in Analysis and Design*, 42(2), 152–168, 2005.

[9] Upadhyay, A.K. and Shukla, K.K., Geometrically nonlinear static and dynamic analysis of functionally graded skew plates, *Communications in Nonlinear Science and Numerical Simulation*, 18(8), 2252-2279, 2013.

[10] Singha, M.K. and Daripa, R., Nonlinear vibration of symmetrically laminated composite skew plates by finite element method, *International Journal of Non-Linear Mechanics*, 42(9), 1144-1152, 2007.

[11] Ganapathia, M. and Prakashb, T., Thermal buckling of simply supported functionally graded skew plates, *Composite Structures*, 74(2), 247-250, 2006.

[12] Nie, G.J. and Zhong, Z., Semi-analytical solution for three-dimensional vibration of functionally graded circular plates, *Computer Methods in Applied Mechanics and Engineering*, 196(49-52), 4901-4910, 2007.

[13] Allahverdizadeh, A., Naei, M.H. and Bahrami, M. N., Nonlinear free and forced vibration analysis of thin circular functionally graded plates, *Journal of Sound and Vibration*, 310(4-5), 966-984, 2008.

[14] Allahverdizadeh, A., Naei, M.H. and Bahrami, M. N., Vibration amplitude and thermal effects on the nonlinear behavior of thin circular functionally graded plates, *International Journal of Mechanical Sciences*, 50(3), 445-454, 2008.

[15] Zhu, P. and Liew, K.M., A local Krigingmeshless method for free vibration analysis of functionally graded circular plates in thermal environments, *International Conference on Advances in Computational Modeling and Simulation Procedia Engineering*, 31, 1089-1094, 2012.

[16] Talabi, M. R. and Saidi, A. R., An explicit exact analytical approach for free vibration of circular/annular functionally graded plates bonded to piezoelectric actuator/sensor layers based on Reddy's plate theory, *Applied Mathematical Modelling*, 37(14-15), 7664-7684, 2013.

[17] Matsunaga, H., Free vibration and stability of functionally graded circular cylindrical shells according to a 2D higher-order deformation theory, *Composite Structures*, 88(4), 519-531, 2009.

[18] Hosseini-HashemiSh., Fadaee M. and Es'haghi, M., A novel approach for in-plane/out-of-plane frequency analysis of functionally graded circular/annular plates, *International Journal of Mechanical Sciences*, 52(8), 1025-1035, 2010.

[19] Patel, B.P., Gupta, S.S., Loknath, M.S. and Kadu, C.P., Free vibration analysis of functionally graded elliptical cylindrical shells using higher-order theory, *Composite Structures*, 69(3), 259-270, 2005.

[20] Hsieh, J. J. and Lee, L. T., An inverse problem for a functionally graded elliptical plate with large deflection and slightly disturbed boundary, *International Journal of Solids and Structures*, 43(20), 5981-5993, 2006.

[21] Zhang, D-G, Non-linear bending analysis of super elliptical thin plates, *International Journal of Non-Linear Mechanics*, 55, 180-185, 2013.

[22] Çeribaşı, S., Altay, G. and Dökmeci, M. C., Static analysis of superelliptical clamped plates by Galerkin's method, *Thin-Walled Structures*, 46(2), 122-127, 2008.

[23] Nie, G.J. and Zhong, Z., Vibration analysis of functionally graded annular sectorial plates with simply supported radial edges, *Composite Structures*, 84(2), 167-176, 2008.

[24] Nie, G. and Zhong, Z., Dynamic analysis of multi-directional functionally graded annular plates, *Applied Mathematical Modelling*, 34(3), 608-616, 2010.

[25] Hosseini-Hashemi, S., Derakhshani, M. and Fadaee, M., An accurate mathematical study on the free vibration of stepped thickness circular/annular Mindlin functionally graded plates, *Applied Mathematical Modelling*, 37(6), 4147-4164, 2013.

[26] Jodaeia, A., Jalalb, M. and Yasa, M.H., Free vibration analysis of functionally graded annular plates by state-space based differential quadrature method and comparative modeling by ANN, *Composites Part B: Engineering*, 43(2), 340-353, 2012.

[27] Ebrahimi, F., Rastgoo, A. and Atai, A.A., A theoretical analysis of smart moderately thick shear deformable annular functionally graded plate, *European Journal of Mechanics - A/Solids*, 28(5), 962-973, 2009.

[28] Tajeddini, V., Ohadi, A. and Sadighi, M., Three-dimensional free vibration of variable thickness thick circular and annular isotropic and functionally graded plates on Pasternak foundation, *International Journal of Mechanical Sciences*, 53(4), 300-308, 2011.

[29] Belalia, S.A. and Houmat, A., Nonlinear free vibration of functionally graded shear deformable sector plates by a curved triangular *p*-element, *European Journal of Mechanics - A/Solids*, 35, 1-9, 2012.

[30] Reddy, J.N., *Mechanics of Laminated Composite Plates and Shells: Theory and Analysis*, CRC Press; 2nd edition, 2004.